中国激光

透明介质材料的超快激光微纳加工研究进展

李佳群[1]，闫剑锋[1*]，李欣[2]，曲良体[1,3]

[1]清华大学机械工程系，北京 100084；

[2]北京理工大学机械车辆学院，北京 100081；

[3]清华大学化学系，北京 100084

摘要 透明介质材料具有高透光性、高耐热性和良好的耐腐蚀性，被广泛应用于航空航天、微电子器件和光学元件等领域，这些应用对透明介质材料微纳加工的精度与质量提出了一定的要求。超快激光具有超高的峰值强度与超短的脉冲持续时间，可突破衍射极限并极小化热影响区，具有出色的加工精度与加工质量，为透明介质材料的微纳尺度加工提供了多样化的手段。综述了透明介质材料的超快激光微纳加工研究进展，包括超快激光加工透明介质材料的内部结构、相关机理和应用领域三个方面，并对透明介质材料的超快激光微纳加工进行了总结与展望。

关键词 激光技术；超快激光；透明介质材料；微纳加工；折射率变化；纳米光栅；纳米孔洞

中图分类号 TN249 **文献标志码** A **doi**：10.3788/CJL202148.0202019

1 引 言

透明介质材料一般指可见光波段透光率在80%以上的材料，如玻璃、宝石、金刚石、部分有机聚合物与各种晶体，其具有高透光性、高机械强度、高耐热性与良好的耐腐蚀能力，在航空航天[1]、微电子器件[2]和柔性光子器件[3]等领域具有广泛的应用。传统手段如机械加工方式容易造成透明介质材料的破碎与崩裂，其精度也难以完全满足微纳尺度的要求。激光作为一种材料适应性广的非接触式加工工具，在透明介质材料的微纳加工方面优势明显。超快激光(脉冲持续时间小于 10 ps)相比于纳秒激光与连续激光，具有更高的加工精度，已成为微纳制造的重要工具之一。超快激光具有超强特性，表现出极高的峰值强度，可突破衍射极限[4]，为微纳米材料加工开辟了新的途径。利用双光子聚合技术可加工出分辨率在 120 nm 左右的三维纳米牛[5]。超快激光具有超快特性，脉冲宽度短于绝大多数物理化学过程的特征时间，能以非热加工的形式完成材料的修饰或去除[6]，在电子将能量传递给晶格建立热平衡之前，激光能量吸收已经结束，极高的峰值功率密度使能量局限在激光作用区域周边小范围内，可极小化热影响区。利用高重复频率的飞秒激光可在牙齿基质与脑组织等结构中进行定点烧蚀，不影响周围区域[7]。随着激光技术的发展，超快激光近十几年来被广泛应用于微电子器件[8]、数据存储与传感器[9]、生物医学工程[10-11]和新能源[12-13]等领域。

本文将从超快激光与透明介质材料的相互作用过程出发，综述超快激光在透明介质材料内部诱导产生的内部结构变化与相关机理，以及透明介质材料超快激光微纳加工在波导和微通道等领域的应用，如图 1 所示。

2 超快激光诱导透明介质材料的内部结构变化

2.1 超快激光与透明介质材料的相互作用过程

图 2 所示为超快激光与透明介质材料的作用过程。如图 2(a)所示，当可见光或近红外波段的超快激光辐照透明介质材料时，由于介质材料本身几乎不含有自由电子，因此材料不吸收激光能量。然而，超快激光具有极高峰值强度，可以通过多光子电离或隧穿电离的方式，将焦点处透明介质材料价带中

收稿日期：2020-08-24；**修回日期**：2020-09-21；**录用日期**：2020-10-14

基金项目：国家重点研发计划（2017YFB1104300）、国家自然科学基金（51775303，52075289）

*E-mail：yanjianfeng@tsinghua.edu.cn

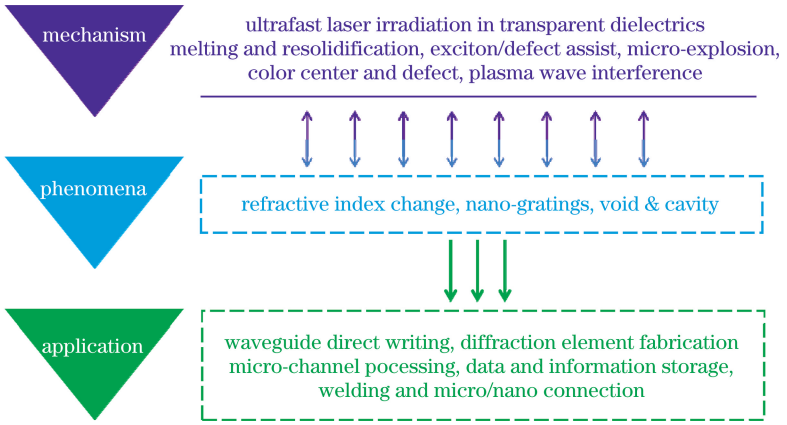

图 1 超快激光加工透明介质的机理、现象与应用

Fig. 1 Mechanisms, phenomena and applications of ultrafast laser processing of transparent dielectrics

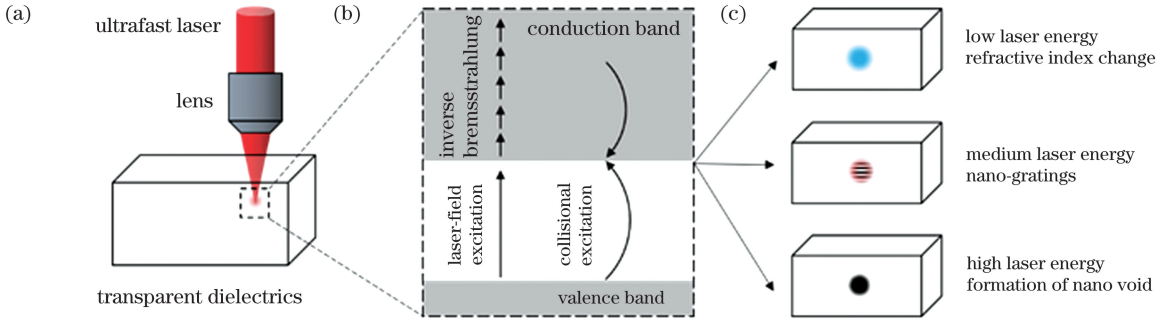

图 2 超快激光与透明介质材料作用过程。(a)超快激光辐照透明介质内部的示意图;(b)透明介质材料中的电子电离过程;(c)不同通量的超快激光在透明介质中引起结构变化

Fig. 2 Interaction between ultrafast laser and transparent dielectrics. (a) Diagram of ultrafast laser irradiation inside transparent dielectrics; (b) electron ionization process in transparent dielectrics; (c) structural changes in transparent dielectrics induced by ultra-fast laser with different fluxes

的束缚电子激发到导带成为自由电子[14-15]。这些被激发到导带的自由电子作为“种子电子”一方面通过逆韧致辐射吸收光子能量,另一方面通过碰撞电离引发电子的“雪崩”,进而以雪崩电离的形式实现对激光能量的吸收,如图 2(b)所示。电子完成超快激光能量的吸收后,再将能量传递给晶格,引起后续透明介质材料的结构与性质变化。图 2(c) 所示为不同通量的超快激光在透明介质中引起结构变化。

2.2 超快激光诱导透明介质材料的内部结构变化

根据聚焦到透明介质材料内部的能量等级,将超快激光在透明介质材料内部诱导产生的结构变化分为三种:低脉冲能量可在介质内部诱导形成折射率变化区域[16],适中的脉冲能量可在透明介质内部诱导产生纳米光栅结构[17],高脉冲能量则会在透明介质材料内部诱导产生纳米孔洞结构[18]。

2.2.1 折射率变化

图 3 所示为超快激光诱导透明介质材料的三种结构变化。如图 3(a)所示,当入射透明介质材料内部的激光能量略微超过改性阈值时,会在材料内部引起折射率的改变,使介质折射率由初始的 n_0 变化为 n_1。受介质材料本身性质与激光辐照参数的影响,折射率的变化数值可正可负,分布可均匀可不均匀。利用 810 nm 波长的飞秒激光聚焦辐照不同组分的玻璃,在辐照区域可观察到折射率增加现象,如图 3(b)所示[19]。

大部分透明介质材料经低能量超快激光辐照后,材料内部产生的折射率变化为正值。例如使用 820 nm 波长、60 fs 脉宽和 1 kHz 重复频率的飞秒激光辐照石英玻璃与掺硼玻璃,石英玻璃被辐照区域的折射率增加了 3×10^{-3},掺硼玻璃的折射率增加值可达 5×10^{-3}[22]。利用飞秒激光对铝硅酸盐玻璃进行辐照,发现多脉冲高重复频率的激光可在玻璃内部产生折射率增加值约为 3×10^{-3} 的波导结构[23]。

少数介质的折射率在超快激光作用后表现出负变化或是非均匀变化的特性。例如,在磷酸盐玻璃中使用 800 nm 波长和 150 fs 脉宽的飞秒激光辐照加工,激光辐照区域出现了折射率减小的情况[24]。

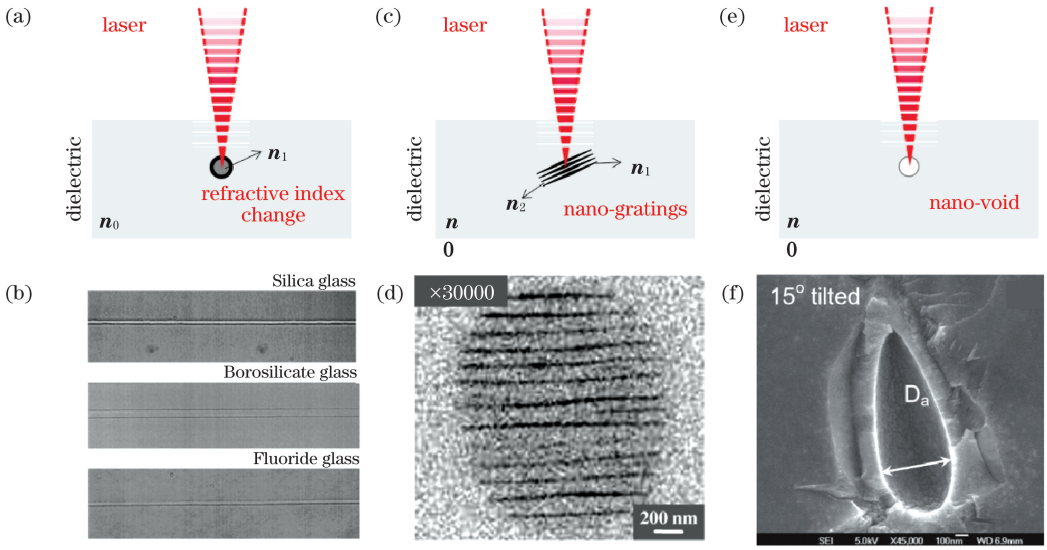

图 3 超快激光诱导透明介质材料的三种结构变化。(a)超快激光诱导折射率变化示意图;(b)超快激光在玻璃中诱导折射率变化直写波导结构[19];(c)超快激光诱导纳米光栅结构示意图;(d)纳米光栅结构的背散射电子图像[20];(e)超快激光诱导纳米孔洞结构示意图;(f)蓝宝石中纳米孔洞的横截面电镜图[21]

Fig. 3 Three structural changes in transparent dielectrics induced by ultrafast laser. (a) Schematic of refractive index change induced by ultrafast laser; (b) waveguide structure directly written via ultrafast laser induced refractive index change[19]; (c) diagram of nanograting structures induced by ultrafast laser; (d) back-scattered electron images of nanograting structures[20]; (e) diagram of nanovoid structures induced by ultrafast laser; (f) cross sectional electron microscopy image of nanovoid sturctures in sapphire[21]

利用飞秒激光辐照数种多组分玻璃,被辐照区域的折射率变化可正可负,也存在着不均匀变化的情况,表现出对成分的强依赖性[25],如表 1 所示,其中 NA 为聚焦物镜的数值孔径。使用多种脉宽的超快激光贝塞尔光束对玻璃进行辐照改性,发现受辐照区域的折射率变化呈由正到负的非均匀分布[26]。

表 1 不同透明材料中超快激光诱导的折射率变化情况

Table 1 Refractive index changes induced by ultrafast laser in different transparent dielectrics

Material	Laser treatment	Refractive index	Reference
Ge-doped silica glass	fs laser with wavelength of 800 nm, pulse duration of 120 fs and repetition rate of 200 kHz	0.01–0.035	[19]
Corning 0211 glass	fs laser with pulse energy of 5 nJ and NA of 1.4	3×10^{-4}	[23]
Corning 7890 glass	fs laser	About 0.0045	[27]
Standard fiber	fs laser with wavelength of 800 nm and pulse duration of 120 fs	6×10^{-3}	[28]
Silica glass	fs laser	About 3×10^{-4}	[22]
Silica glass	fs laser with pulse duration of 130 fs and repetition rate of 1 kHz	8×10^{-3}	[29]
IOG-1 glass	fs laser with pulse duration of 130 fs and wavelength of 800 nm	-1.4×10^{-4}	[24]
BK7 glass	fs laser	About -0.004 ± 0.0001	[25]
Lithium-borosilicate glass	fs laser	About -0.0003 ± 0.0002	[25]
Schott glass 8261	fs laser	About 0.003 ± 0.0002	[25]
Alkali-aluminum-silicate glass	fs laser	About 0.0004(edge) and about -0.0012 ± 0.0002 (center)	[25]
LAS glass	fs laser	About 1.5×10^{-3}	[25]
Lead-silicate glass SF57	fs laser	About 0.003 ± 0.0002	[25]
Corning glass	fs laser (Bessel beam)	Non-uniform	[26]

2.2.2 纳米光栅结构

如图 3(c)所示，当入射透明介质材料的激光能量超过改性阈值但小于光学击穿阈值时，可在介质内部诱导形成一种呈周期性片层状分布的纳米光栅结构，其折射率与基体材料不同，导致被辐照区域双折射率发生变化。使用 130 fs 脉宽和 200 kHz 重复频率的飞秒激光辐照熔融石英，发现在辐照区域产生了永久的各项异性双折射率改变[30]。在锗掺杂的熔融石英中，通过飞秒激光辐照同样得到了反常各向异性光散射结构，其散射强度在光偏振平面上达到峰值[31]。利用飞秒激光辐照稀土金属掺杂的石英玻璃，也观察到这种与偏振相关的光散射现象，这是超快激光本身的偏振性质导致了这种永久的偏振依赖性光散射结构[32]。借助扫描电子显微镜对辐照区域进行分析，在图 3(d)的背散射电子图像中发现了垂直于激光偏振方向宽度约为 20 nm 的条纹状周期性纳米结构，该结构表现出低氧浓度的特点[20]。通过原子力显微镜与扫描电子显微镜，发现氢氟酸对这种偏振敏感的纳米光栅结构表现出强烈的选择性刻蚀，氧元素浓度较低的暗条纹区域的刻蚀速率远高于其余部分[33]。

2.2.3 纳米孔洞结构

如图 3(e)所示，当入射透明介质材料的激光峰值强度较高时(超过 10^{14} W/cm^2)，辐照中心会产生极高的温度与压强，引发的微爆炸冲击波使聚焦区域向外膨胀，在中心形成被致密化介质包围的纳米孔洞结构或低密度区域。使用高能量的单脉冲飞秒激光对蓝宝石、玻璃和聚合物等透明介质材料进行辐照，发现被辐照区域中生成了纳米尺度孔洞结构[34]。使用 800 nm 波长和 180 fs 脉宽的飞秒激光单脉冲，在石英玻璃中得到纳米孔洞结构，该结构产生的主要原因是冲击波与稀疏波的作用[35]。使用飞秒激光单脉冲也可在蓝宝石内部制造出高压(10 TPa)与高温(0.5 MK)的极端条件，被辐照区域的材料在极短时间内就出现等离子体，继而在远超任何材料强度的高压状态下，生成冲击波与稀疏波，导致图 3(f)中纳米孔洞结构的形成[21]。对橄榄石进行飞秒激光单脉冲辐照处理，激光导致的微爆炸使橄榄石内部形成了纳米孔洞结构。微爆炸影响区域周围结构的近边 X 射线吸收谱显示出现了一种新晶相，激光影响区域的拉曼光谱则显示晶格出现有序性的降低并生成了混合纳米晶[36]。

3 超快激光诱导透明介质材料结构变化的分析

3.1 折射率变化

图 4 为超快激光诱导透明介质材料结构变化相关机制。利用原位拉曼散射光谱对飞秒激光辐照后的熔融石英改性区域结构变化进行分析，拉曼光谱中出现了两个较大幅度的峰值增加(490 cm^{-1} 处与 605 cm^{-1} 处)，表明在激光辐照后，通过多元环的转化，石英网络结构中的四元环与三元环的数量增多，如图 4(a)所示，因此硅氧键键角的减小意味着在激光辐照影响的折射率变化区域中出现了石英结构的致密化[37]。通过原子力显微镜观察 810 nm 波长飞秒激光在熔融石英中直写的波导结构，发现激光辐照区域出现了表面收缩，收缩幅度随着离辐照区域中心距离的减小而增大[38]。有关超快激光辐照透明介质诱导折射率变化过程的机理解释主要有热致熔化与重凝和色心诱导等。

3.1.1 热致熔化与重凝

利用 25 MHz 重复频率的飞秒激光对玻璃进行辐照处理，通过调节同一点上累积的脉冲个数，可在纳焦量级上实现对沉积能量的控制，进而影响改性区域的范围。分析认为，激光非线性能量吸收引起的热积累导致局部熔化，局部熔化在玻璃折射率变化过程中起到了主要作用，即激光焦点作为一个可移动的极小热源，在材料内部引起的局部熔化与重新凝固导致辐照区域折射率发生改变[41]。使用有限差分热模拟方法，验证了 200 kHz 重复频率以上的飞秒激光在加工铝硅酸盐玻璃时出现的热量积累效应，发现热积累量和激光净通量之间存在函数关系[42]。在 250 kHz 重复频率的飞秒激光辐照玻璃的实验中，通过分析热积累的温度分布与热改性的特征温度，发现激光辐照区域存在热量积累与扩散，且温度分布规律与应力分布规律基本一致[43]。

3.1.2 色心诱导

色心指的是晶体中能对可见光产生选择性吸收的缺陷部位。利用 850 nm 波长的飞秒激光辐照玻璃，在低于烧蚀阈值的激光通量下辐照区域有色心的产生[44]。通过飞秒激光辐照磷酸玻璃，在共聚焦显微镜发光光谱结果中也观察到了激光辐照中心区域有色心形成，且该部分区域折射率相比于初始值有轻微降低[22]。使用低能量的振荡级激光与高能量的放大级激光辐照玻璃，前者引起的温度变化可以忽略，后者有1000 ℃以上的改变，二者的折射率

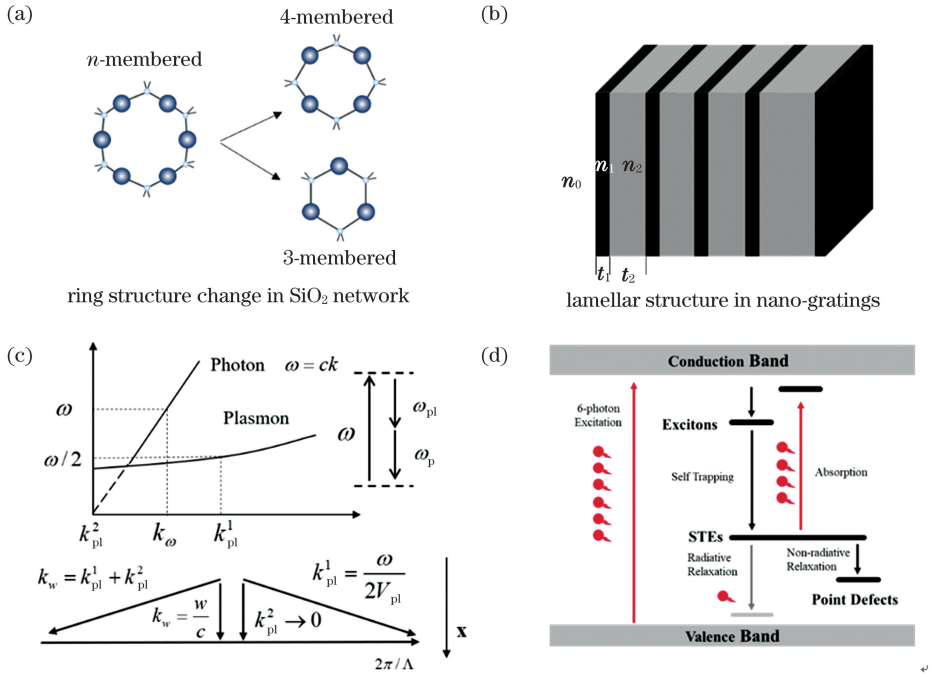

图 4 超快激光诱导透明介质材料结构变化相关机制。(a)激光辐照玻璃引起 SiO_2 结构变化;(b)纳米光栅结构的简单模型;(c)双等离子体激元衰减模型[39];(d)自陷激子与半永久点缺陷形成过程[40]

Fig. 4 Mechanism of ultrafast laser induced structural changes in transparent dielectrics. (a) Structural change of SiO_2 induced by laser irradiation; (b) simple model of nanograting structure; (c) dual plasmon decay model[39]; (d) self-trapping exciton and semi-permanent point defect formation process[40]

变化却基本一致,该结果并不支持热积累效应,同时还发现介质折射率的变化与色心浓度的变化具有相同趋势[45]。利用磷酸玻璃上的布拉格光栅作为诊断工具,观测光漂白与热退火过程中微小的折射率变化,发现超快激光辐照区域中的色心在介质折射率的变化以及波导结构直写过程中起到了作用[46]。

3.2 纳米光栅结构

图 4(b)所示的是纳米光栅结构的一个简单模型,其主要由两层折射率不同且沿激光偏振方向呈周期性排列的片状结构组成,因此表现出与激光偏振垂直的特性。其中厚度较小、折射率为 n_1 的区域具有较多氧缺陷,表现出低氧浓度,折射率相比未加工区域降低了约 0.1[47],主要由多孔玻璃组成[48]。另一层厚度较大且折射率为 n_2 的部分,主要由嵌入了纳米晶的石英层组成,该纳米晶可能是由压力波与温度升高的共同作用引起的[49]。有关超快激光诱导产生纳米光栅结构的机理主要有入射光场与等离子体波电场的干涉、纳米等离子体的非对称生长及激子与缺陷辅助形成等。

3.2.1 入射光场与等离子体波电场的干涉

入射激光与透明介质材料作用时,通过非线性电离过程产生大量自由电子,极高的自由电子密度使激光辐照区域出现等离子体态,等离子体对激光能量的吸收主要是通过逆韧致辐射进行的,并引发了纵向的等离子体波。等离子体波的电场在入射光偏振平面上与光场发生耦合干涉,导致等离子体密度发生周期性调制,并最终在材料中形成与偏振相关的周期性结构变化[20]。基于上述单等离子体激发的双等离子体激元衰减模型如图 4(c)所示,当两束等离子体中的一束用于传播且另一束与其共振时,发生的互相干涉可导致亚波长纳米结构的生成,此时等离子体波频率与共振频率基本一致,且两束等离子体密度均低于原本的单束等离子体密度,使得在 10^4 K 的低电子温度下也能产生纳米光栅结构[39]。

3.2.2 纳米等离子体的非对称生长

当超快激光辐照透明介质材料内部时,介质内部本身存在的缺陷或色心可作为多光子电离的电离热点。受到后续数个激光脉冲的作用,这些电离热点通过某种反馈机制逐渐演化成球形的纳米等离子体。在增强的边界电场作用下,纳米等离子体会发生非对称生长(偏向垂直于激光偏振方向),从纳米球变成纳米椭球体,逐渐形成盘状等离子体,在增强的等离子体边缘场作用下,盘状等离子体逐步合并

为纳米面。随着激光能量的继续输入，等离子体的电子密度增加至临界电子密度，这些纳米面呈现出金属化特征，与入射光产生干涉并影响入射光传播，最后以一定的周期排布在聚焦区域内，形成纳米光栅结构[50]。

3.2.3 激子与缺陷辅助纳米结构形成

在纳米等离子体非对称生长模型中，纳米光栅的形成需要多个脉冲协同作用，但在多脉冲激光的脉冲间隔时间长于等离子体寿命时，也观察到了纳米光栅结构的生成。图 4(d)所示的基于激子与缺陷辅助的纳米光栅结构的形成理论可以解释这一现象。根据脉冲间隔时间的长短，可将该过程分为两类：当脉冲间隔短于激子寿命时，辐照区域被激发的自由电子被晶格捕获后形成自陷激子，在激光脉冲结束后一段时间内，自陷激子仍然存在，这种激子中的电子被激发到导带所需要的能量更低，更易被后续激光脉冲电离，加快了材料吸收激光的效率，有助于多脉冲作用下纳米光栅结构的生成；在脉冲间隔长于激子寿命的情况下，辐照区域所形成的自陷激子会衰变为半永久的点缺陷，这些点缺陷在后续激光脉冲作用下为激光能量吸收提供了种子电子，与自陷激子类似，降低了材料吸收激光能量的门槛，增加了多脉冲作用下纳米光栅结构生成的效率[40]。

3.3 纳米孔洞结构

使用高能量激光紧聚焦辐照透明介质表层边界 15 μm 以下区域，结合实验观测与理论模型，可对超快激光辐照透明介质材料产生微爆炸并生成纳米尺度孔洞结构的过程作出解释。当超快激光被紧聚焦于透明材料内部约 0.3 μm^3 的空间时(与表层距离大于 15 μm，远大于入射激光波长)，会产生高功率密度的光场，通过多光子电离以及雪崩电离过程，此部分透明介质出现光学击穿现象，其光学性质发生巨大变化。随后在 1/6 μm^3 的吸收体积内产生了强烈的激光能量吸收，能量密度达到 5.6×10^6 J/cm^3，压力超出材料所能承受的强度值三个数量级，引起向外传播的强烈膨胀冲击波与向焦点内部传播的稀疏波。冲击波会压缩吸收体积周围的物质，波前后方被压缩的材料在巨大压强作用下急剧转变为另一种相，在压强被释放后，受冲击波影响的区域迅速转变为常压下的最终相。在向焦点内部传播的稀疏波的作用下，焦点体积中心则会产生孔洞结构，使用高分辨电子显微镜观察到该孔洞的尺寸约为 500 nm。基于两相流体动力学方程与状态方程，可对孔洞的体积以及激光影响区域的尺寸大小进行模拟与预测，预测结果与实验结果基本一致[51]。

4 透明介质材料的超快激光微纳加工应

使用超快激光对透明介质材料进行辐照处理，通过熔化重凝、微爆炸和缺陷形成等过程，可产生以折射率变化、纳米光栅结构和纳米孔洞这三种现象为代表的结构变化。以此为基础，利用超快激光在透明介质材料中能直写制备出多种器件与结构，并应用于光波导[52]、衍射光学元件[53]、微孔[54]与微通道[55]等领域。

4.1 光波导器件直写

光波导与其相关器件的直写是透明介质材料超快激光微纳加工的应用领域之一。光波导的加工通常采用物镜聚焦激光在介质材料内部进行移动直写，包括纵向直写与横向直写两种形式。前者具有规则的圆形加工区域，但受到物镜工作距离的限制，能够加工的波导结构长度有限；后者则可进行任意长度的波导结构制备，加工的最高深度取决于所采用的物镜的工作距离，但在横向直写时，需要通过引入狭缝等光场整形手段，才能实现圆形波导结构的加工。

使用 800 nm 波长、120 fs 脉宽的超快激光结合空间光整形技术，可在玻璃内部实现三维空间分裂光波导结构的制备[52]。为解决直写过程中两个聚焦光斑距离太近导致的干涉现象，通过在空间光调制器上加载特殊相位，将直写前后聚焦光斑的距离进行解耦，使光斑间的距离增大以避免干涉发生，最终得到 1×4 的分裂光波导结构，该结构的分光比经测试为 28∶23∶25∶24，只有约 16%的激光能量由于分光过程出现了损失[56]。如图 5(a)所示，通过 795 nm 波长、120 fs 脉宽的飞秒激光直写加工 Ho∶$KGd(WO_4)_2$ 晶体，在激光加工区域引起了 -6×10^{-4} 的负折射率变化，将这些低折射率区域在圆周上排布，可形成直径约为 60 μm 的埋入式波导结构，其传播损耗经测试为(0.94±0.2) dB/cm，且在连续波工作模式下该结构的斜率效率可达 67.2%[57]。图 5(b)所示则是通过 515 nm 波长、3.15 MHz 重复频率的飞秒激光在蓝宝石中直写的凹层光波导结构，该结构被一圈激光诱导的低折射率区域(折射率相比于未加工区域低 1×10^{-3}～5.3×10^{-3})所包围，传播损耗经测试低至 0.37 dB/cm[58]。

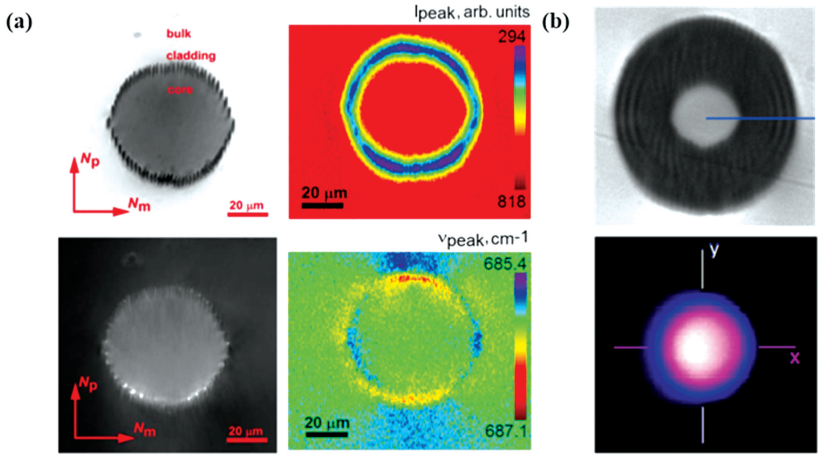

图 5 超快激光直写的波导器件。(a)飞秒激光脉冲直写的埋入式波导结构[57];(b)飞秒激光加工的凹层波导结构[58]

Fig. 5 Waveguide devices directly written by ultrafast laser. (a) Embedded waveguide structure directly written by femtosecond laser pulse [57]; (b) depressed cladding waveguide structure processed by femtosecond laser[58]

4.2 衍射光学元件加工

衍射光学元件主要用于光束整形与分束的研究。利用聚焦超快激光在透明介质材料中直写产生的折射率变化、双折射率变化以及纳米孔洞等现象，可制备衍射光栅、衍射透镜和全息图像等衍射光学元件。例如使用 300 fs 脉宽的飞秒激光在铌酸锂晶体中直写制备体积布拉格光栅，其衍射效率随着光栅厚度的增加可达 87%，并在 150 ℃的温度下热退火 1 h 仍然保持不变[59]。

飞秒激光辐照结合化学刻蚀在熔融石英上制备的微透镜如图 6(a)所示。该加工过程中使用的飞秒激光双脉冲序列可以调控熔融石英被辐照区域的局部瞬时自由电子密度，使辐照区域的光致改性得到优化和增强，二氧化硅网络中的三元环与四元环结构显著增加，伴随着 Si—O—Si 键角的减小，氧原子活性增强，化学刻蚀效率提高至 37 倍[60]。在熔融石英中还可借助超快激光直写来加工菲涅耳区板、偏振转换器和几何棱镜透镜等元件。使用飞秒激光选择性修饰熔融石英表面同心圆环的双折射率，可实现菲涅耳区板的直写加工，该元件衍射效率经测试为 39%，接近理论上菲涅耳区板作为相位透镜的 40% 的最大效率[61]。图 6(b)所示的是飞秒激光在熔融石英中制备的几何相位棱镜与几何相位透镜。通过 300 fs 脉宽、200 kHz 重复频率的飞秒激光，在石英中直写制备了沿垂直偏振方向延伸的纳米孔；利用该各向异性纳米多孔二氧化硅，通过飞秒激光诱导制备了纳米光栅结构；通过调控辐照区域的双折射率，可实现对入射圆偏振光的传播方向及聚焦散焦的调控[62]。

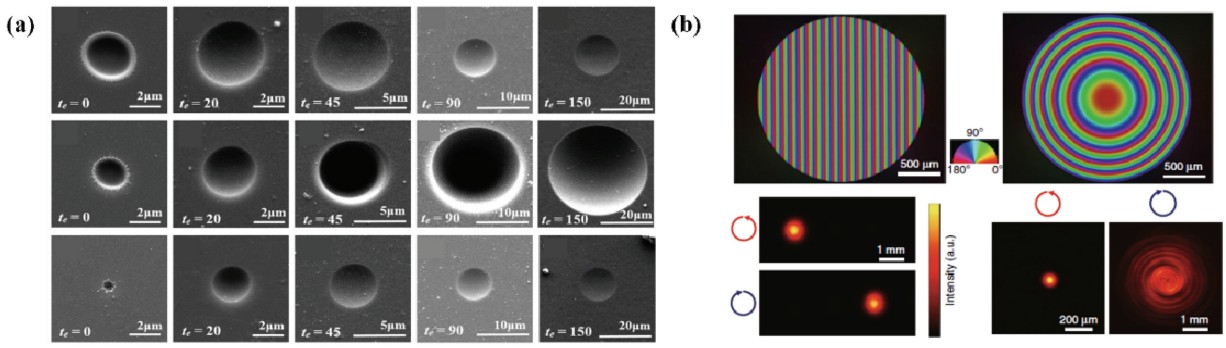

图 6 超快激光制备的衍射光学元件。(a)飞秒激光脉冲序列辐照熔融石英制备微透镜[60];(b)飞秒激光加工的几何相位棱镜与几何相位透镜[62]

Fig. 6 Diffraction optical elements prepared by ultrafast laser. (a) Microlens prepared by femtosecond laser pulse train irradiating of fused silica substrate[60]; (b) geometric phase prisms and lens prepared by femtosecond laser[62]

4.3　微孔与微通道制备

超快激光在透明介质材料中加工的微通道与微孔已应用于微流体器件、芯片实验室和电子封装等领域，可用作样本分析、物质检测和反应合成等。目前，超快激光加工透明介质材料微孔与微通道的方法主要有激光直接烧蚀、激光背向湿法刻蚀与激光辅助化学湿法刻蚀三种，如图 7 所示。激光直接烧蚀是通过单脉冲加工、多脉冲叩击式加工、环切加工或螺旋加工等方式来实现自上而下或自下而上的材料去除，借助微爆炸和烧蚀等过程直接制备微孔和微通道结构。激光诱导背向湿法刻蚀利用介质材料在液体中具有更低的烧蚀阈值这一特点，在溶液中完成材料自下而上的逐层去除，利用辅助液体带走烧蚀过程中产生的热量以及碎屑残渣，实现高质量的微孔与微通道结构加工。激光辅助化学湿法刻蚀方法则是利用激光在透明介质内部预先形成折射率变化或纳米光栅等改性结构，在这些结构的基础上利用改性前后刻蚀速率的差异实现微孔与微通道的制备。

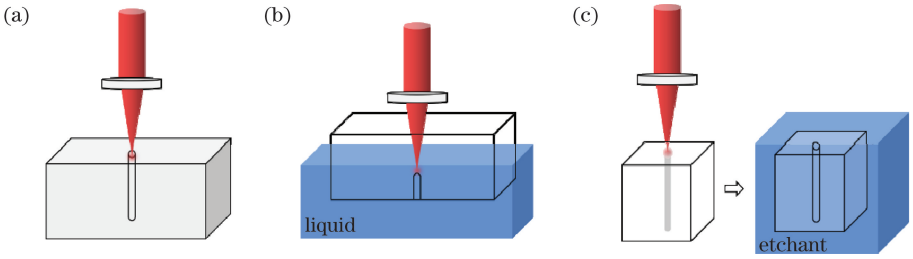

图 7　超快激光微孔微通道制备方法。(a)激光直接烧蚀；(b)激光诱导背向湿法刻蚀；(c)激光辅助的化学湿法刻蚀

Fig. 7　Method for preparing micro-hole and microchannel with ultrafast laser. (a) Direct laser ablation; (b) laser induced backside wet etching; (c) laser assisted chemical wet etching

超快激光加工的微孔与微通道如图 8 所示。将空间高斯分布的飞秒激光整形成贝塞尔光束，通过控制空间局部瞬时自由电子密度，可在聚甲基丙烯酸甲酯(PMMA)材料中得到图 8(a)所示的无锥度、深径比为 560∶1 的微通道结构[55]。通过脉冲整形器来调节三阶色散与二阶色散系数，将 785 nm 波长、30 fs 脉宽的时域高斯分布脉冲整形成为时域艾利分布递减脉冲以及时域展宽脉冲，如图 8(b)所

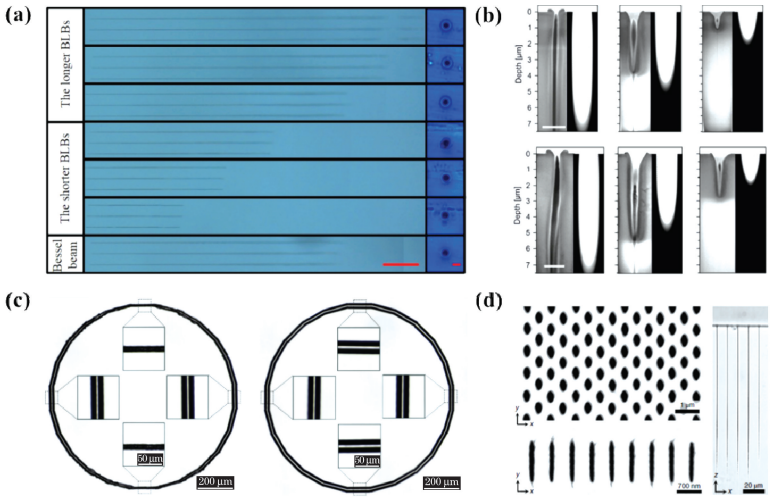

图 8　超快激光加工的微孔与微通道。(a)类贝塞尔光束微通道加工结果(长度标尺为 100 μm，直径标尺为 2 μm)[55]；(b)时域艾里分布光束与时域展宽光束微孔加工结果[63]；(c)补偿球差效应前后使用飞秒激光加工的环形微通道结构[64]；(d)钇铝石榴石晶体经飞秒激光辅助化学刻蚀得到的微孔阵列结构[65]

Fig. 8　Micro-holes and microchannels processed by ultrafast laser. (a) Micro-channel processing results by Bessel-like beam(length scale bar is 100 μm, and diameter scale bar is 2 μm)[55]; (b) micro-hole processing results by temporal Airy beam and temporally broadened beam[63]; (c) annular micro-channel structures processed by femtosecond laser before and after compensation of spherical aberration effect[64]; (d) micro-hole array obtained by femtosecond laser-assisted chemical etching of yttrium aluminum garnet crystal[65]

示，利用单个脉冲在熔融石英中制备得到直径为 250 nm、深径比为 30∶1 的超衍射极限微孔结构[63]。基于空间光调制器补偿球差效应带来的飞秒激光聚焦深度差异，实现了精确可控的圆形截面加工，在聚甲基丙烯酸甲酯(PMMA)材料中制备出图 8(c)所示的直径均匀一致的内部环形微通道结构[64]。使用 1030 nm 波长、350 fs 脉宽的线偏振飞秒激光，在钇铝石榴石晶体中进行改性直写加工，辅以磷酸进行化学湿法刻蚀，得到了图 8(d)所示的孔径约为 200 nm 的微孔阵列结构[65]。

利用飞秒激光双脉冲加工 PMMA 材料，得到的微孔结构如图 9(a)所示，在相同激光通量下，右图的双脉冲加工结果相比于左图单脉冲加工结果，其深度提升了 1/5，深径比提升了 1/6。通过调节飞秒激光贝塞尔光束的光场分布，可实现图 9(b)所示的深径比达到 1000∶1 的微通道制备，该微通道直径约为 1.5 μm，深度达到 1.5 mm。使用飞秒激光诱导背向湿法刻蚀，得到的微通道加工结果如图 9(c)所示，其直径小于 5 μm，深度大于 1100 μm，深径比达到 260∶1。

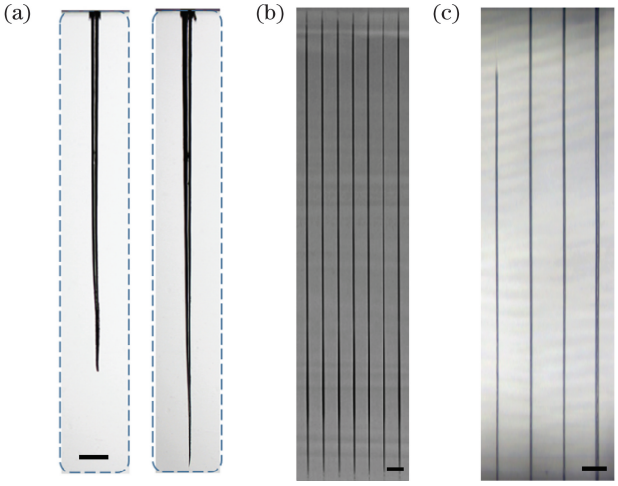

图 9 本课题组使用超快激光加工的微孔与微通道。(a)双脉冲飞秒激光增加微孔烧蚀深度(标尺为 100 μm)；(b)贝塞尔单脉冲加工的微通道，图中标尺为 10 μm；(c)硼硅玻璃中激光诱导背向湿法刻蚀得到的微通道，图中标尺为 40 μm

Fig. 9 Micro-holes and microchannels processed by ultrafast laser in our research group. (a) Enhancement of ablation depth by femtosecond laser double pulses (scale bar is 100 μm); (b) micro-channel processed by single Bessel pulse (scale bar is 10 μm); (c) micro-channel processed by laser induced backside wet etching in borosilica glass (scale bar is 40 μm)

文献[66-78]报道的微通道直径和长度分布如图 10 所示，其中 A 点对应图 9(b)所示的微通道，B 点对应图 9(c)所示的微通道。对于激光直接烧蚀的加工结果，其直径与深度可覆盖较大范围，小到数百纳米，大到 20 μm，也是三种加工方式中最容易实现纳米尺寸微通道的方法。激光诱导背向湿法刻蚀方法加工的微通道直径与微孔直径则趋于中间水平，尤其是在加工 5 μm 直径左右的微通道时，该方法表现出直接烧蚀与激光辅助化学刻蚀所不具备的优势，直接烧蚀在该直径下难以实现高深径比，而激光辅助化学刻蚀难以控制刻蚀程度，直径容易扩大。激光辅助化学湿法刻蚀方法在制备大直径(数十微米以上)以及更大深度微通道与微孔方面具有优势，例如使用飞秒激光聚焦改性石英玻璃，结合氢氧化钾溶液的选择刻蚀性，加工得到的微通道直径可达 50 μm，长度达到 1 cm，深径比约为 200∶1[79]。

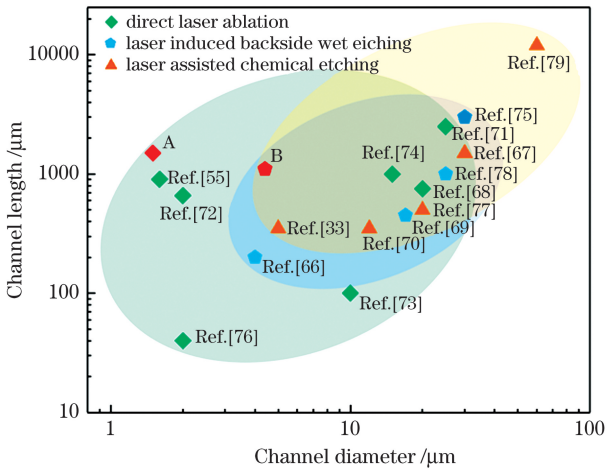

图 10 微通道直径和长度分布[66-78]

Fig. 10 Distributions of micro-channel diameter and length [66-78]

4.4 数据与信息存储

超快激光在透明介质材料中诱导的结构与性质变化可与未加工区域形成“0”与“1”的二值对比，按照需求将“0”与“1”的结构阵列集成在透明介质中并应用于数据与信息存储领域。

利用基于透明介质的超快激光微纳加工方法，可开发一种由三维的空间维度与二维的光学维度所组成的永久五维信息存储方法。以飞秒激光与玻璃作用后形成的纳米光栅结构为基础，除去三维空间维度外，将慢轴方向作为第四个维度，迟滞强度(双折射率和结构长度的乘积)作为第五个维度，通过控制激光强度和偏振对这两个额外维度进行调控，可

实现图案化加工与信息存储功能[80]。利用飞秒激光原位诱导结晶技术，含有 Cs，Pb 和 Br 等元素的基体玻璃经激光辐照后，在辐照区域生成 $CsPbBr_3$ 钙钛矿量子点，该量子点具有较低的形成能，会很快解离，经过后续的低温退火，可以重新生成并保持稳定，利用二次激光辐照与退火过程可实现此种量子点的擦除与复写，起到数据信息存储与保密的作用[81]。通过飞秒激光辐照掺银氟磷酸盐玻璃，在辐照区域可生成银纳米团簇与银纳米粒子。基于此现象可以实现具有强烈荧光对比度的 3D 微米级图案化结构直写，且这些结构可以通过后续激光的重叠辐照等过程实现擦除与重写，在 3D 高密度光学数据存储方面具有一定的应用潜力[82]。

4.5 微纳连接与焊接

当超快激光辐照透明介质材料时，通过受激的非线性过程与多光子吸收过程，辐照区域会出现强烈的能量吸收。基于这一性质，在需要连接的界面处，通过聚焦超快激光可实现同种或异种材料的连接。实验获取了不同脉冲重复频率和不同脉冲能量下玻璃吸收超快激光能量后的强度、非线性吸收率和温度分布情况，将该结果应用于片状玻璃材料的微焊接，可得到基本没有裂纹的连接结果[83]。通过热处理调节陶瓷透光性，得到晶粒尺寸在 100 nm 左右的透明陶瓷，该陶瓷对超快激光具有低散射强吸收的特点，因此超快激光能深入聚焦到材料内部而不会被表面散射，相比于传统陶瓷连接需要在全局高温环境下进行，该方法可在室温下完成对陶瓷电子封装结构的超快激光焊接，所得结果的抗剪切强度与传统扩散连接相近[84]。

5 结束语

综述了超快激光在透明介质材料内部诱导产生的内部结构变化与相关机理，介绍了透明介质材料超快激光微纳加工在波导、衍射光学元件和微孔微通道等领域的应用。根据激光辐照能量的高低，超快激光诱导透明介质材料内部产生的结构变化分为折射率变化（低）、纳米光栅（中）与纳米孔洞结构（高）。基于超快激光诱导结构变化的微纳器件制备方法在透明介质材料的微纳加工应用领域已展现出优势。透明介质材料的超快激光微纳加工研究有助于人们理解介质材料与激光的相互作用过程，有利于基于超快激光诱导折射率变化和纳米光栅结构等现象的微纳加工应用领域的拓展，拥有广阔与光明的前景。随着超快激光技术的不断发展以及对超快激光微纳加工过程的深入理解，透明介质材料的超快激光微纳加工研究会取得新的进展，在航空航天、生物医学和能源工程等领域发挥更大的作用。

参 考 文 献

[1] Li J, Jiang N, Xu S Q, et al. Resent development on infrared transparent MgO-Y_2O_3 nanocomposite ceramics[J]. Journal of the Chinese Ceramic Society, 2016, 44(9): 1302-1314.
李江, 姜楠, 徐圣泉, 等. 红外透明 MgO-Y_2O_3 纳米复相陶瓷研究进展[J]. 硅酸盐学报, 2016, 44(9): 1302-1314.

[2] Fu Y P, Cai X, Wu H W, et al. Fiber supercapacitors utilizing pen ink for flexible/wearable energy storage[J]. Advanced Materials, 2012, 24(42): 5713-5718.

[3] Ye Y T, Ma H, Sun C L, et al. Research progress on flexible photonic materials and devices[J]. Laser & Optoelectronics Progress, 2020, 57(3): 030001.
叶羽婷, 马辉, 孙春雷, 等. 柔性光子材料与器件的研究进展[J]. 激光与光电子学进展, 2020, 57(3): 030001.

[4] McMillen B, Zhang B T, Chen K P, et al. Ultrafast laser fabrication of low-loss waveguides in chalcogenide glass with 0.65 dB/cm loss[J]. Optics Letters, 2012, 37(9): 1418-1420.

[5] Kawata S, Sun H B, Tanaka T, et al. Finer features for functional microdevices[J]. Nature, 2001, 412(6848): 697-698.

[6] Sugioka K, Cheng Y. Ultrafast lasers: reliable tools for advanced materials processing[J]. Light: Science & Applications, 2014, 3(4): e149.

[7] Kerse C, KalaycIoğlu H, Elahi P, et al. Ablation-cooled material removal with ultrafast bursts of pulses[J]. Nature, 2016, 537(7618): 84-88.

[8] Ji L F, Ma R, Zhang X M, et al. Application of laser lift-off technique in flexible electronics manufacturing[J]. Chinese Journal of Lasers, 2020, 47(1): 0100001.
季凌飞, 马瑞, 张熙民, 等. 激光剥离技术在柔性电子制造领域的应用研究进展[J]. 中国激光, 2020, 47(1): 0100001.

[9] Zhong M L, Fan P X. Applications of laser nano manufacturing technologies[J]. Chinese Journal of Lasers, 2011, 38(6): 0601001.
钟敏霖, 范培迅. 激光纳米制造技术的应用[J]. 中国激光, 2011, 38(6): 0601001.

[10] Hu P X, Yao L, Lü Q T, et al. Ultra-fast laser milling technology for VITA MARK Ⅱ dental glass ceramics[J]. Laser & Optoelectronics Progress, 2020, 57(5): 051402.

胡培鑫, 姚路, 吕启涛, 等. VITA MARK Ⅱ牙科玻璃陶瓷超快激光铣削工艺[J]. 激光与光电子学进展, 2020, 57(5): 051402.

[11] Yu J C, Jiang L, Yan J F, et al. Microprocessing on single protein crystals using femtosecond pulse laser [J]. ACS Biomaterials Science & Engineering, 2020, 6(11): 6445-6452.

[12] Qiao M, Yan J F, Gao B. Ablation of TiO_2 surface with a double-pulse femtosecond laser [J]. Optics Communications, 2019, 441: 49-54.

[13] Qiao M, Yan J F, Qu L T, et al. Femtosecond laser induced phase transformation of TiO_2 with exposed reactive facets for improved photoelectrochemistry performance [J]. ACS Applied Materials & Interfaces, 2020, 12(37): 41250-41258.

[14] Bloembergen N. A brief history of light breakdown [J]. Journal of Nonlinear Optical Physics & Materials, 1997, 6(4): 377-385.

[15] Stuart B C, Feit M D, Rubenchik A M, et al. Laser-induced damage in dielectrics with nanosecond to subpicosecond pulses [J]. Physical Review Letters, 1995, 74(12): 2248-2251.

[16] Apostolopoulos V, Laversenne L, Colomb T, et al. Femtosecond-irradiation-induced refractive-index changes and channel waveguiding in bulk Ti^{3+}: sapphire [J]. Applied Physics Letters, 2004, 85(7): 1122-1124.

[17] Ramirez L P R, Heinrich M, Richter S, et al. Tuning the structural properties of femtosecond-laser-induced nanogratings [J]. Applied Physics A, 2010, 100(1): 1-6.

[18] Juodkazis S, Vailionis A, Gamaly E G, et al. Femtosecond laser-induced confined microexplosion: tool for creation high-pressure phases [J]. MRS Advances, 2016, 1(17): 1149-1155.

[19] Miura K, Qiu J R, Inouye H, et al. Photowritten optical waveguides in various glasses with ultrashort pulse laser [J]. Applied Physics Letters, 1997, 71(23): 3329-3331.

[20] Shimotsuma Y, Kazansky P G, Qiu J R, et al. Self-organized nanogratings in glass irradiated by ultrashort light pulses [J]. Physical Review Letters, 2003, 91(24): 247405.

[21] Juodkazis S, Nishimura K, Tanaka S, et al. Laser-induced microexplosion confined in the bulk of a sapphire crystal: evidence of multimegabar pressures [J]. Physical Review Letters, 2006, 96(16): 166101.

[22] Homoelle D, Wielandy S, Gaeta A L, et al. Infrared photosensitivity in silica glasses exposed to femtosecond laser pulses [J]. Optics Letters, 1999, 24(18): 1311-1313.

[23] Schaffer C B, Brodeur A, García J F, et al. Micromachining bulk glass by use of femtosecond laser pulses with nanojoule energy [J]. Optics Letters, 2001, 26(2): 93-95.

[24] Chan J W, Huser T R, Risbud S H, et al. Waveguide fabrication in phosphate glasses using femtosecond laser pulses [J]. Applied Physics Letters, 2003, 82(15): 2371-2373.

[25] Bhardwaj V R, Simova E, Corkum P B, et al. Femtosecond laser-induced refractive index modification in multicomponent glasses [J]. Journal of Applied Physics, 2005, 97(8): 083102.

[26] Bhuyan M K, Velpula P K, Colombier J P, et al. Single-shot high aspect ratio bulk nanostructuring of fused silica using chirp-controlled ultrafast laser Bessel beams [J]. Applied Physics Letters, 2014, 104(2): 021107.

[27] Streltsov A M, Borrelli N F. Fabrication and analysis of a directional coupler written in glass by nanojoule femtosecond laser pulses [J]. Optics Letters, 2001, 26(1): 42-43.

[28] Fertein E, Przygodzki C, Delbarre H, et al. Refractive-index changes of standard telecommunication fiber through exposure to femtosecond laser pulses at 810 cm [J]. Applied Optics, 2001, 40(21): 3506-3508.

[29] Yamada K, Watanabe W, Toma T, et al. *In situ* observation of photoinduced refractive-index changes in filaments formed in glasses by femtosecond laser pulses [J]. Optics Letters, 2001, 26(1): 19-21.

[30] Sudrie L, Franco M, Prade B, et al. Writing of permanent birefringent microlayers in bulk fused silica with femtosecond laser pulses [J]. Optics Communications, 1999, 171(4/5/6): 279-284.

[31] Kazansky P G, Inouye H, Mitsuyu T, et al. Anomalous anisotropic light scattering in Ge-doped silica glass [J]. Physical Review Letters, 1999, 82(10): 2199-2202.

[32] Qiu J R, Kazanski P G, Si J H, et al. Memorized polarization-dependent light scattering in rare-earth-ion-doped glass [J]. Applied Physics Letters, 2000, 77(13): 1940-1942.

[33] Hnatovsky C, Taylor R S, Simova E, et al. Fabrication of microchannels in glass using focused femtosecond laser radiation and selective chemical etching [J]. Applied Physics A, 2006, 84(1/2): 47-61.

[34] Gamaly E G, Juodkazis S, Nishimura K, et al. Laser-matter interaction in the bulk of a transparent solid: Confined microexplosion and void formation

[J]. Physical Review B, 2006, 73(21): 214101.

[35] Juodkazis S, Misawa H, Hashimoto T, et al. Laser-induced microexplosion confined in a bulk of silica: formation of nanovoids[J]. Applied Physics Letters, 2006, 88(20): 201909.

[36] Buividas R, Gervinskas G, Tadich A, et al. Phase transformation in laser-induced micro-explosion in olivine (Fe, $Mg)_2SiO_4$ [J]. Advanced Engineering Materials, 2014, 16(6): 767-773.

[37] Chan J W, Huser T, Risbud S, et al. Structural changes in fused silica after exposure to focused femtosecond laser pulses[J]. Optics Letters, 2001, 26(21): 1726-1728.

[38] Hirao K, Miura K. Writing waveguides and gratings in silica and related materials by a femtosecond laser [J]. Journal of Non-Crystalline Solids, 1998, 239(1/2/3): 91-95.

[39] Misawa H. 3D laser microfabrication: principles and applications[M]. Hoboken : John Wiley & Sons, Inc., 1999.

[40] Richter S, Heinrich M, Döring S, et al. Nanogratings in fused silica: formation, control, and applications[J]. Journal of Laser Applications, 2012, 24(4): 042008.

[41] Schaffer C B, García J F, Mazur E. Bulk heating of transparent materials using a high-repetition-rate femtosecond laser[J]. Applied Physics A: Materials Science & Processing, 2003, 76(3): 351-354.

[42] Eaton S, Zhang H B, Herman P, et al. Heat accumulation effects in femtosecond laser-written waveguides with variable repetition rate[J]. Optics Express, 2005, 13(12): 4708-4716.

[43] Sakakura M, Shimizu M, Shimotsuma Y, et al. Temperature distribution and modification mechanism inside glass with heat accumulation during 250 kHz irradiation of femtosecond laser pulses[J]. Applied Physics Letters, 2008, 93(23): 231112.

[44] Efimov O M, Gabel K, Garnov S V, et al. Color-center generation in silicate glasses exposed to infrared femtosecond pulses [J]. Journal of the Optical Society of America B, 1998, 15(1): 193-199.

[45] Streltsov A M, Borrelli N F. Study of femtosecond-laser-written waveguides in glasses[J]. Journal of the Optical Society of America B, 2002, 19(10): 2496-2504.

[46] Dekker P, Ams M, Marshall G D, et al. Annealing dynamics of waveguide Bragg gratings: evidence of femtosecond laser induced colour centres[J]. Optics Express, 2010, 18(4): 3274-3283.

[47] Bricchi E, Kazansky P G. Extraordinary stability of anisotropic femtosecond direct-written structures embedded in silica glass[J]. Applied Physics Letters, 2006, 88(11): 111119.

[48] Lancry M, Poumellec B, Canning J, et al. Ultrafast nanoporous silica formation driven by femtosecond laser irradiation[J]. Laser & Photonics Reviews, 2013, 7(6): 953-962.

[49] Oliveira V, Sharma S P, Herrero P, et al. Transformations induced in bulk amorphous silica by ultrafast laser direct writing [J]. Optics Letters, 2013, 38(23): 4950-4953.

[50] Taylor R, Hnatovsky C, Simova E. Applications of femtosecond laser induced self-organized planar nanocracks inside fused silica glass [J]. Laser & Photonics Reviews, 2008, 2(1/2): 26-46.

[51] Hallo L, Mézel C, Bourgeade A, et al. Laser-matter interaction in transparent materials: confined micro-explosion and jet formation [M]// Hall T J, Gaponenko S V, Paredes S A. Extreme photonics & applications. NATO science for peace and security series B: physics and biophysics. Dordrecht: Springer, 2010: 121-146.

[52] Morris J M, MacKenzie M D, Petersen C R, et al. $Ge_{22}As_{20}Se_{58}$ glass ultrafast laser inscribed waveguides for mid-IR integrated optics[J]. Optical Materials Express, 2018, 8(4): 1001.

[53] Voigtländer C, Richter D, Thomas J, et al. Inscription of high contrast volume Bragg gratings in fused silica with femtosecond laser pulses [J]. Applied Physics A, 2011, 102(1): 35-38.

[54] Qiao M, Wang H M, Lu H J, et al. Micro/nano processing of natural silk fibers with near-field enhanced ultrafast laser[J]. Science China Materials, 2020, 63(7): 1300-1309.

[55] Yao Z L, Jiang L, Li X W, et al. Non-diffraction-length, tunable, Bessel-like beams generation by spatially shaping a femtosecond laser beam for high-aspect-ratio micro-hole drilling[J]. Optics Express, 2018, 26(17): 21960-21968.

[56] Sakakura M, Sawano T, Shimotsuma Y, et al. Fabrication of three-dimensional 1 × 4 splitter waveguides inside a glass substrate with spatially phase modulated laser beam [J]. Optics Express, 2010, 18(12): 12136-12143.

[57] Kifle E, Loiko P, Romero C, et al. Femtosecond-laser-written Ho∶$KGd(WO_4)_2$ waveguide laser at 2.1 μm[J]. Optics Letters, 2019, 44(7): 1738-1741.

[58] Bérubé J P, Lapointe J, Dupont A, et al. Femtosecond laser inscription of depressed cladding single-mode mid-infrared waveguides in sapphire[J]. Optics Letters, 2019, 44(1): 37-40.

[59] Paipulas D, Kudriašov V, Malinauskas M, et al. Diffraction grating fabrication in lithium niobate and KDP crystals with femtosecond laser pulses [J]. Applied Physics A, 2011, 104(3): 769-773.

[60] Zhao M J, Hu J, Jiang L, et al. Controllable high-throughput high-quality femtosecond laser-enhanced chemical etching by temporal pulse shaping based on electron density control[J]. Scientific Reports, 2015, 5(1): 13202.

[61] Beresna M, Gecevičius M, Kazansky P G. Polarization sensitive elements fabricated by femtosecond laser nanostructuring of glass [J]. Optical Materials Express, 2011, 1(4): 783-795.

[62] Sakakura M, Lei Y H, Wang L, et al. Ultralow-loss geometric phase and polarization shaping by ultrafast laser writing in silica glass [J]. Light: Science & Applications, 2020, 9: 15.

[63] Götte N, Winkler T, Meinl T, et al. Temporal Airy pulses for controlled high aspect ratio nanomachining of dielectrics[J]. Optica, 2016, 3(4): 389.

[64] Roth G L, Rung S, Esen C, et al. Microchannels inside bulk PMMA generated by femtosecond laser using adaptive beam shaping [J]. Optics Express, 2020, 28(4): 5801-5811.

[65] Ródenas A, Gu M, Corrielli G, et al. Three-dimensional femtosecond laser nanolithography of crystals[J]. Nature Photonics, 2019, 13(2): 105-109.

[66] Li Y, Itoh K, Watanabe W, et al. Three-dimensional hole drilling of silica glass from the rear surface with femtosecond laser pulses[J]. Optics Letters, 2001, 26(23): 1912-1914.

[67] Maselli V, Osellame R, Cerullo G, et al. Fabrication of long microchannels with circular cross section using astigmatically shaped femtosecond laser pulses and chemical etching[J]. Applied Physics Letters, 2006, 88(19): 191107.

[68] Zhao X, Shin Y C. Femtosecond laser drilling of high-aspect ratio microchannels in glass[J]. Applied Physics A, 2011, 104(2): 713-719.

[69] Jiang L, Liu P, Yan X, et al. High-throughput rear-surface drilling of microchannels in glass based on electron dynamics control using femtosecond pulse trains[J]. Optics Letters, 2012, 37(14): 2781-2783.

[70] Wang Z, Jiang L, Li X W, et al. High-throughput microchannel fabrication in fused silica by temporally shaped femtosecond laser Bessel-beam-assisted chemical etching[J]. Optics Letters, 2018, 43(1): 98-101.

[71] Xia B, Jiang L, Li X, et al. Mechanism and elimination of bending effect in femtosecond laser deep-hole drilling [J]. Optics Express, 2015, 23(21): 27853-27864.

[72] Xie Q, Li X W, Jiang L, et al. High-aspect-ratio, high-quality microdrilling by electron density control using a femtosecond laser Bessel beam [J]. Applied Physics A, 2016, 122(2): 1-8.

[73] Ito Y, Yoshizaki R, Miyamoto N, et al. Ultrafast and precision drilling of glass by selective absorption of fiber-laser pulse into femtosecond-laser-induced filament[J]. Applied Physics Letters, 2018, 113(6): 061101.

[74] Karimelahi S, Abolghasemi L, Herman P R. Rapid micromachining of high aspect ratio holes in fused silica glass by high repetition rate picosecond laser [J]. Applied Physics A, 2014, 114(1): 91-111.

[75] Yoshiki K. High-aspect ratio laser drilling of glass assisted by supercritical carbon dioxide [J]. Proceedings of SPIE, 2017, 1009: 100921K.

[76] Bhuyan M K, Courvoisier F, Lacourt P A, et al. High aspect ratio taper-free microchannel fabrication using femtosecond Bessel beams[J]. Optics Express, 2010, 18(2):566-574.

[77] Sun Q, Saliminia A, Théberge F, et al. Microchannel fabrication in silica glass by femtosecond laser pulses with different central wavelengths [J]. Journal of Micromechanics & Microengineering, 2008, 18(3):035039.

[78] Hwang D J, Choi T Y, Grigoropoulos C P. Liquid-assisted femtosecond laser drilling of straight and three-dimensional microchannels in glass[J]. Applied Physics A, 2004, 79(3):605-612.

[79] Kiyama S, Matsuo S, Hashimoto S, et al. Examination of etching agent and etching mechanism on femotosecond laser microfabrication of channels inside vitreous silica substrates [J]. Journal of Physical Chemistry C, 2015, 113(27):11560-11566.

[80] Zhang J, Čerkauskaité A, Drevinskas R, et al. Eternal 5D data storage by ultrafast laser writing in glass [J]. Proceedings of SPIE, 2016, 9736: 97360U.

[81] Huang X, Guo Q, Yang D, et al. Reversible 3D laser printing of perovskite quantum dots inside a transparent medium[J]. Nature Photonics, 2020, 14(2):1-7.

[82] Castro T D, Fares H, Khalil A A, et al. Femtosecond laser micro-patterning of optical properties and functionalities in novel photosensitive silver-containing fluorophosphate glasses[J]. Journal of Non-Crystalline Solids, 2019, 517(517):51-56.

[83] Miyamoto I, Cvecek K, Okamoto Y, et al. Internal

modification of glass by ultrashort laser pulse and its application to microwelding[J]. Applied Physics A, 2014, 114(1):187-208.

[84] Penilla E H, Devia-Cruz L F, Wieg A T, et al. Ultrafast laser welding of ceramics[J]. Science, 2019:803-808.

Research Advancement on Ultrafast Laser Microprocessing of Transparent Dielectrics

Li Jiaqun[1], Yan Jianfeng[1*], Li Xin[2], Qu Liangti[1, 3]

[1] *Department of Mechanical Engineering, Tsinghua University, Beijing* 100084, *China*;

[2] *School of Mechanical Engineering, Beijing Institute of Technology, Beijing*, 100081, *China*;

[3] *Department of Chemistry, Tsinghua University, Beijing* 100084, *China*

Abstract

Significance Transparent dielectrics generally refer to materials with a transmittance of more than 80% in the visible light range, such as glass, gemstones, diamonds, some organic polymers, and various crystals. They have been extensively used in aerospace, electronic elements, flexible photonic devices, and other advanced fields because of their high transmittance and corrosion resistance. However, processing transparent dielectrics with traditional methods like mechanical physical means in the micro-nano scale is rather difficult because they can easily cause breakage and cracks.

With ultrahigh intensity and ultrashort pulse duration, an ultrafast laser (pulse duration $<$10 ps) can break the diffraction limit due to its wide material adaptability and extreme precision and can minimize the heat-affected zone, providing an advanced approach for micro-nano fabrication. Hence, an ultrafast laser has become the most appropriate tool for the micro-nano fabrication of transparent dielectrics. The corresponding phenomena and physical mechanisms in the ultrafast laser fabrication of transparent materials must be investigated to optimize the micro-nano scale processing of transparent dielectrics and utilize it in more application fields.

Progress The structural changes induced by the ultrafast laser in the irradiation area can be divided into three types according to the different pulse energy levels focused inside the transparent dielectrics: 1) low pulse energy can induce the formation of areas where the refractive index change occurs inside the dielectrics, 2) under moderate pulse energy, a nanograting structure can be induced, and 3) high pulse energy induces a nanovoid structure at the irradiation point.

If the energy of the laser incident into transparent dielectrics slightly exceeds the modification threshold, the structural change in the irradiation area will be induced, which causes the refractive index to change from the initial n_0 to n_1(Fig. 3). As for this structural change, there exist two mainstream explanations. Some scholars believe that the local melting and re-solidification play a major role due to the heat accumulation caused by nonlinear laser energy absorption, and the other studies have proven that the color center accounts for the refractive index change.

If the energy of the pulse incident into transparent dielectrics exceeds the material′s modification threshold, but is less than the optical breakdown threshold, the formation of a nanograting structure will be induced, which consists of multiple layers of materials with different refractive indexes and thus it results in the birefringent change of the irradiation area. The mechanism behind this phenomenon can be explained in three ways: some studies believe that the interference between the incident laser and induced plasma accounts for the nanograting formation, some studies attribute the structural change to the asymmetric growth of the nanoplasma, and the other studies think excitons and defect assistance play a more pivotal part in the nanograting′s evolution.

When the peak intensity of the incident laser is higher than 10^{14} W·cm^{-2}, the high energy density and the electromagnetic field will cause an optical breakdown of transparent dielectrics. The optical properties of the irradiated area will also be greatly changed. Meanwhile, extremely high temperature and pressure will be engendered in the center of the irradiation area. A strong expansion shock wave propagating outward and a sparse wave propagating inside the focal point will be generated under such extreme conditions. The shock wave compresses the material around the absorption volume, and the sparse wave creates a void structure in the center of the focal volume.

Numerous applications of transparent dielectrics have been implemented based on these three structural changes induced by an ultrafast laser. For instance, optical waveguides can be directly written in materials with a refractive index increase or decrease. Diffractive optical elements can be fabricated by laser regulating dielectric birefringence or chemical etching after irradiation. Micro-holes and micro-channels can be produced by direct ablation, laser-induced backside wet etching, and laser-assisted chemical etching. Information and data storage can be achieved by the unique feature difference between processed and unprocessed areas like refractive index and structural color. A micro-nano-connection can be realized by local melting and resolidification at the interface of two dielectrics under a suitable energy ultrafast pulse irradiation.

Conclusion and Prospect Interm of the incident laser energy, three types of structural changes are induced by ultrafast lasers in transparent materials: refractive index changes, nanogratings, and nanovoids. The micro-nano device preparation method developed based on the ultrafast laser-induced structural changes has shown advantages and potentials in the application of the micro-nano fabrication of transparent dielectrics. Research on the ultrafast laser micro-nano processing of transparent dielectrics can not only help understand the interaction between dielectric materials and lasers, but also provide various applications in the micro-nano field based on the phenomena such as ultrafast laser-induced refractive index changes and nanograting structures. With the continuous development of the ultrafast laser technology and an in-depth understanding of the ultrafast laser micro-nano fabrication process, research on the ultrafast laser micro-nano processing of transparent materials will make a new progress in aerospace, biomedicine, energy engineering, and other fields.

Key words laser technique; ultrafast laser; transparent dielectrics; micro-nano processing; refractive index change; nanogratings; nanovoids

OCIS codes 140.3390; 130.3990; 130.2755